2021

Thermodynamic Comparison of Transcritical Carbon Dioxide Booster Architectures to an R-513A Booster System in Commercial Refrigeration

David Snyder
Chemours, United States of America, david.snyder@chemours.com

Andrew Pansulla

Charles Allgood

Thermodynamic Comparison of Transcritical Carbon Dioxide Booster Architectures to an R-513A Booster System in Commercial Refrigeration

David SNYDER[1]*, Andrew PANSULLA[2], Charles ALLGOOD[3]

[1]The Chemours Company, Fluorochemicals,
Newark, DE, United States of America
Tel. 302-773-6669, david.snyder@chemours.com

* Corresponding Author

ABSTRACT

As global regulatory framework has been introduced to phase down the manufacture and use of hydrofluorocarbon (HFC) refrigerants on a total carbon emissions basis, many end users have been tasked with finding alternatives to current refrigeration architectures and associated working fluids. Using commercial refrigeration as an example, transcritical R-744 (CO_2) booster architectures have been studied, piloted, and compared to conventional R-404A centralized systems. Many studies show favorable energy consumption and COP (coefficient of performance) in colder climates for CO_2 versus R-404A. Concurrent with the advances in CO_2 technology is the development of the lower GWP (global warming potential) HFC alternative of hydrofluoroolefins (HFO). This paper discusses the development and use of thermodynamic cycle models for a transcritical CO_2 booster system and an R-513A booster system in commercial refrigeration. Base system architectures were compared as well as upgrades to these systems including parallel compression, ejectors, and adiabatic condensers.

Optimization schemes were used for system COP, gas cooler pressure, flash tank intermediate pressure, and ejector motive nozzle outlet pressure. A correction factor was applied for the medium and low temperature case loads to account for the influence of outdoor air temperature (OAT). Additionally, while a standard approach temperature was used for the modeled R-513A condenser, CO_2 gas cooler outlet temperatures were calculated using published experimental correlations to OAT to provide a fair comparison. Weather data from twelve select cities of differing climate zones and moisture regimes in the United States were used in conjunction with a selected set of system inputs representing typical commercial refrigeration operation. Comparison plots of both total compressor energy consumption and combined system COP as a function of ambient temperature were used to compare the various architectures. Total yearly compressor energy consumption by system type at each of the studied locations was also reported.

1. INTRODUCTION

In response to the implementation of refrigerant regulations such as F-gas in Europe, the SNAP rules in the USA, and the Kigali amendment globally, the HVACR industry has had to pivot to invent and commercialize new refrigerants and new system architectures to meet the rapid demand for HVACR solutions with lower environmental footprints. One key metric many of the global regulations use to define what refrigerants are acceptable is the GWP. GWP is a qualitative measure of the atmospheric lifetime of a chemical relative to CO_2. However, the GWP of a refrigerant is only one component of the total system carbon emissions. Indirect emissions from electricity usage to operate mechanical refrigeration systems can often exceed the direct carbon emissions from leaking a high GWP refrigerant into the atmosphere. This paper will compare the energy use of CO_2 (AR5 GWP = 1) versus R-513A (AR5 GWP = 573) in booster architectures using multiple ambient temperature profiles. R-513A was selected due to its relatively low GWP for a fluorinated refrigerant and the ability to operate at positive pressures for coil temperatures -29.6 °C (-21.2 °F) and above. All system architectures were optimized as defined in sections 2 through 4.

2. SYSTEM ARCHITECTURES

The base system architectures seen in Figure 1 include medium temperature (MT) and low temperature (LT) compressors, a condenser (also referred to a gas cooler when in supercritical CO_2 operation), an intermediate heat exchanger (IHX) for condenser outlet subcooling and MT compressor suction superheating, MT evaporator, and LT evaporator. The CO_2 system also employs a flash tank which separates the flash gas from the saturated liquid refrigerant prior to entering the evaporator expansion valves.

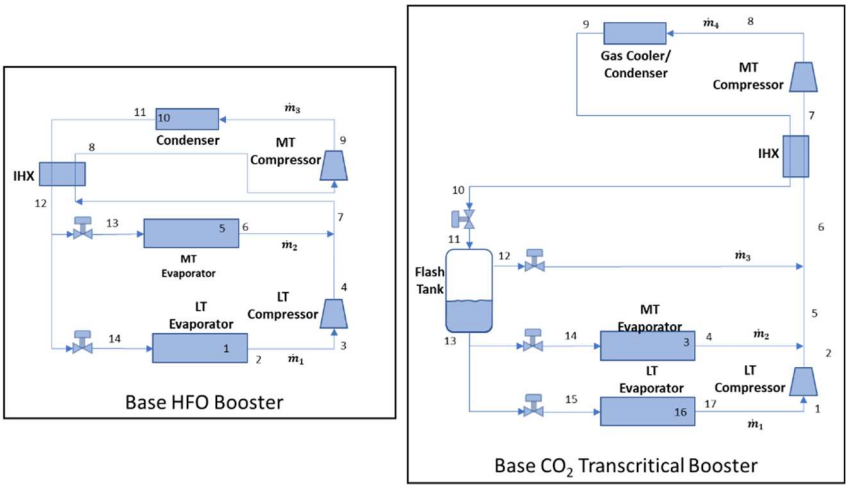

Figure 1: Base System Architectures

Upgrades considered for the base CO_2 transcritical booster system seen in Figure 2 include the use of parallel compressors, ejectors, and adiabatic condensers. While heat recovery and mechanical subcooling are additional areas of interest, they are not the focus of this study.

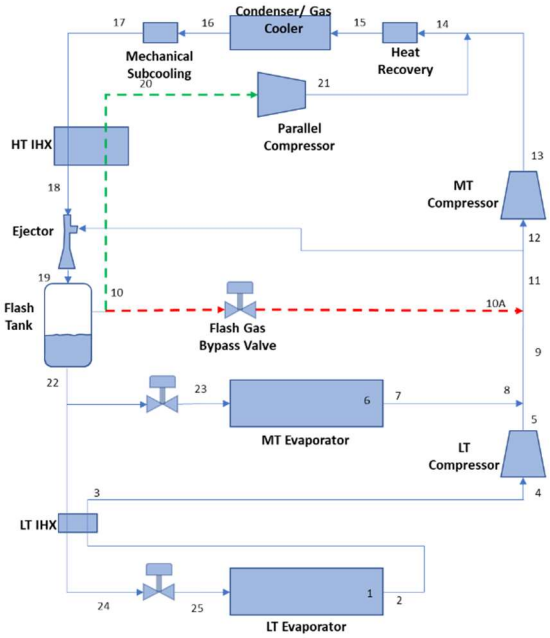

Figure 2: CO_2 Transcritical Booser with Parllel Compression and Ejectors

3. GENERAL ASSUMPTIONS, SYSTEM INPUTS, AND CONSTRAINTS

In the spirit of conducting a fair comparison between refrigerants, details about specific system components were kept as generic as possible. Namely, the following assumptions were made for all models:

- Isenthalpic expansion process
- Pressure drop in all components was neglected
- System operation was considered at steady state conditions
- Heat transfer between system components and surroundings was neglected
- No defrost systems or cycles were considered
- The power consumption of condenser fans, controls, and other ancillary devices was neglected
- No consideration was made for charge size or using multiple packaged units to serve the total load
- 24/7 operation with no differentiation between day and night load other than OAT compensation
- An evaporator load correction factor was applied to adjust for OAT effects on store temperature and humidity

3.1 Compressor Considerations

The maximum allowable compressor discharge pressures were set at the appropriate piping allowable pressure ratings. For refrigerant grade copper, this value was assumed to be 46 bar (~667 psia) (Shilliday, 2012). For CO_2 piping, this value was assumed to be 120 bar (~1740 psi) (Emerson, 2014). Maximum discharge temperature for both systems was assumed to be 149°C (300°F). Rather than defining a specific compressor or even a type of compressor and calculating isentropic efficiencies based on pressure ratios for each ambient condition studied, a constant efficiency of 0.65 was used for all compressors. Finally, all compressors were assumed to be variable-speed with adequate turndown to accommodate the range of ambient temperatures studied.

3.2 Condenser Considerations

HFO condenser approach temperatures were kept at a constant 8.3K (15R) for all scenarios (Walker, 2001). Conversely, CO_2 approach temperatures were correlated to OAT through expressions developed by Mitsopoulos *et al.* (2019). The base HFO system minimum condensing temperature was set to 20°C (68°F) in line with Shilliday (2012), Ge and Tassou (2010), and Zhang (2016). When modeling the upgraded HFO system, minimum condensing temperature was reduced to 10°C (50°F). This is attainable using appropriate system components including compressor modulation, variable speed condenser fan control, and electronic expansion valves (Saunders and Knapke, 2013). The CO_2 system minimum condensing temperature was set to 8°C (46.4°F) per Mitsopoulos *et al.* (2019). Condenser subcooling was not specifically assigned due to the use of an IHX. However, the condenser outlet condition was assumed to be saturated liquid. Condenser pressure for the HFO system was calculated based on a given average condensing temperature. Condenser pressure for subcritical CO_2 system operation was calculated as the saturated pressure at a given condenser outlet temperature. The base CO_2 system model in supercritical operation optimized condenser pressure by maximizing the system COP. The upgraded CO_2 system model optimized condenser pressure by minimizing the parallel compressor power since the modeled parallel compressor required significantly more power than the medium or low temperature compressors.

3.3 Evaporator Considerations

Medium temperature was defined as -6.7°C (20°F) while low temperature was defined as -28.9°C (-20°F) to closely match assumptions made by Ge and Tassou (2010), Mitsopoulos *et al.* (2019), Shilliday (2012), Sharma *et al.* (2014), Tsamos *et al.* (2017), and Walker (2001). Evaporator load factors were used to de-rate the required MT and LT loads based on OAT. This correlation was made by Walker (2001) and others (Faramarzi and Walker, 2004; Nelson *et al.,* 2015; Zhang, 2016). The load factor calculations can be seen in Table 1.

Table 1: Load factor calculations

Ambient Temp Range	MT Load	LT Load
<4.4°C (40°F)	MT Load = 0.66*(Design Load)	LT Load = 0.8*(Design Load)
4.4°C (40°F) < Tamb < 29.4°C (85°F)	MT Load = (Load factor)*(Design Load)	LT Load = (Load factor)*(Design Load)
> 29.4°C (85°F)	MT Load = Design Load	LT Load = Design Load

Load Factor is defined in Equation 1:

$$Load\ Factor = 1 - (1 - \min)\left(\frac{85 - OAT}{85 - 40}\right) \quad (1)$$

Where "min" is 0.66 for MT and 0.8 for LT and "OAT" is in degrees Fahrenheit. Design evaporator loads were set to 70.3 kW (20 Tons) for MT and 17.6 kW (5 Tons) for LT assuming an average supermarket size per Shilliday (2012). Suction superheat values were not specifically defined due to the use of an IHX. Evaporator exit conditions were assumed to be saturated vapor.

3.4 Ejector Considerations (CO_2 model only)

Motive, suction, and diffuser nozzle efficiencies were kept constant at 0.8, 0.8, and 0.75 respectively as defined by Liu (2014) and Sarkar (2012). Based on these efficiencies and the conditions studied, compressor power was found to have an optimal motive nozzle outlet pressure of approximately 2.76 MPa (400 psia).

3.5 IHX System Considerations

IHX were modeled for both the HFO and CO_2 systems. System impacts of the IHX were unique for each architecture and set of input conditions. Effectiveness values between 0 to 0.7 were assigned to these exchangers to maximize system performance (Sharma *et al.*, 2014).

4. MODEL DEVELOPMENT

Twelve locations representing different ASHRAE climate zone and moisture regime combinations were considered using ASHRAE's Weather Data Viewer DVD, Version 6.0 (ASHRAE, 2017). Temperature bins of 2.8°C (5°F) were used in this study. System conditions were modeled using the NIST REFPROP 10 application for Microsoft Excel (Lemon *et al.,* 2018).

4.1 HFO Booster Cycle Model

For HFO adiabatic condenser modeling, condensing temperatures were calculated by adding 85 percent of the mean coincident wet bulb temperature per Bhatia (2014) to the same approach temperature used in the air-cooled model. Adiabatic control was assumed to be in effect for OAT of 21°C (70°F) and above. Below 21°C, the dry bulb temperature was used to calculate average condensing temperature.

The MT and LT evaporator pressures were calculated using the inputs of average evaporator temperature, evaporator inlet temperature, and dew point temperature. A goal seek routine was employed to iterate these calculations until a pressure was found where the average between the dew point temperature and the evaporator inlet temperature equaled the desired average evaporator temperature.

IHX outlet temperatures were calculated using an assumed exchanger effectiveness as follows:

$$t_2 = t_1 + E(T_1 - t_1) \quad (2)$$

$$T_2 = T_1 - C(t_2 - t_1) \quad (3)$$

Where t_1 is the evaporator exit temperature before the IHX (state 7 in Figure 1), t_2 is the IHX outlet into the compressor, T_1 is the condenser outlet before the IHX, T_2 is the IHX outlet into the expansion valve, E is the IHX effectiveness, and C is the ratio of thermal capacitances as defined in Equation 4 (Janna, 2010).

$$C = \frac{(\dot{m}C_p)_{min}}{(\dot{m}C_p)_{max}} < 1 \quad (4)$$

Within this cycle were three distinct mass flowrates. The first was the LT evaporator flow calculated using Equation 5.

$$\dot{m} = \frac{\dot{Q}}{(h_{out} - h_{in})} \tag{5}$$

Where $\dot{Q}$ is the evaporator load, h_{out} is the evaporator outlet enthalpy, and h_{in} is the evaporator inlet enthalpy. The mass flowrate through the MT evaporator was calculated using the same equation. Finally, the mass flowrate through the condenser for this cycle was calculated as the sum of the low and medium temperature evaporator flows.

When determining state points throughout the cycle, an issue arose where mass flows were needed to calculate the enthalpy at the mixture of the LT compressor and the MT evaporator outlet (i.e. state 7 in the HFO model). However, this same enthalpy was needed to calculate additional state points which were used to find mass flowrates. To get around this circular reference, an initial guess was made for the ratio between MT and LT mass flowrates. This guess was used to calculate the enthalpy at state 7, which in turn was used to find the total mass flowrate through the system. The ratio of mass flowrates was then reevaluated, and the initial guess was iterated to converge with the calculated value.

Model outputs consisted of MT and LT COP, combined COP, MT and LT theoretical displacement, MT and LT volumetric cooling capacity, and MT and LT compressor power. Combined COP was calculated using Equation 6.

$$COP = \frac{\dot{m}_1(h_2 - h_{14}) + \dot{m}_2(h_6 - h_{13})}{\dot{m}_1\left(h_{4_{actual}} - h_3\right) + \dot{m}_3(h_{9_{actual}} - h_8)} \tag{6}$$

Where $\dot{m}$ stands for flowrate and h for enthalpy. The subscripts in Equation 6 pertain to the HFO diagram in Figure 1. The enthalpy values at the exit of the compressors are designated "actual" to account for the input of compressor efficiency. Compressor power values were calculated using mass flowrates and enthalpy differences between suction and discharge conditions.

4.2 CO_2 Base Transcritical Booster Cycle Model

The system inputs for the CO_2 base transcritical booster cycle are the same as the HFO cycle outside of considerations for the condenser. For this model, the condenser input is the desired exit temperature. These temperatures were calculated for the range of OAT considered using equations from Mitsopoulos *et al.* (2019).

Table 2: Correlations for the calculation of gas cooler outlet temperature

Ambient temperature range [°C]	Condenser/gas cooler outlet temperature [°C]
$T_{amb} \leq 2$	8
$2 < T_{amb} \leq 14$	$T_{amb} + 6$
$14 < T_{amb} \leq 27$	$0.7692(T_{amb}) + 9.23$
$T_{amb} > 27$	Tamb + 3

The critical point of CO_2 is 7.38 MPa and 30.98°C (1070 psia and 87.76°F). Below this point (i.e. subcritical operation), the condenser exit pressure was calculated as the saturated liquid pressure at the input condenser outlet temperature. For supercritical operation, gas cooler pressure was optimized to maximize the calculated system COP.

A circular reference between enthalpy and flowrate calculations also existed in this case. Like the HFO model, an initial guess for LT to MT evaporator mass flowrate ratio was iterated until the model converged. The evaporator mass flowrates were calculated using Equation 5. The mass flowrate through the condenser was calculated using Equation 7.

$$\dot{m}_4 = \frac{(\dot{m}_1 + \dot{m}_2)}{(1 - Quality_{11})} \tag{7}$$

The quality at state 11 (inlet of flash tank) was determined using the state 11 enthalpy and pressure. The pressure at state 11 was set as a constant value of 35 bar (507.63 psia) for all scenarios in the base CO_2 model (Tsamos *et al.,* 2017). This value represents a minimum pressure differential to maintain across the MT expansion valve considering

the MT evaporator pressure. Due to the introduction of a flash tank, an additional flow of saturated vapor out of the flash tank and into the discharge stream from the LT compressor and MT evaporator was present. This flow was calculated as the total flow through the condenser minus the flows through the LT and MT evaporators.

The combined system COP was determined using an expression from Ge and Tassou (2010).

$$COP_{combined} = \frac{y(1-x)(h_4 - h_{14}) + (1-y)(1-x)(h_{17} - h_{15})}{\left(h_{8_{actual}} - h_7\right) + (1-y)(1-x)\left(h_{2_{actual}} - h_1\right)} \quad (8)$$

Where y is the ratio of MT flow to flow through the LT and MT evaporators and x is the quality at state 11.

4.3 CO_2 Transcritical Booster Cycle Model with Parallel Compression and Ejectors

Manufacturers have introduced several upgrades to the original transcritical booster system architecture attempting to combat efficiency loss with increasing OAT. One upgrade is the use of parallel compressors to pump vapor from the flash tank to the condenser pressure thereby reducing the power requirements for the MT compressors. Another upgrade is the use of ejectors to recover losses related to expansion. Adiabatic condensers are also being employed which utilize a water pump to wet pads located near the condenser refrigerant coils which cool the incoming air down near the ambient wet bulb temperature.

To define the state points in this system setup, several values were simultaneously calculated and iterated to converge on a solution. These included ejection ratio, ejector exit quality, ratio of mass flow between LT and MT, and flash tank pressure. One point to note is that the intermediate pressure of the flash tank was dependent on the performance calculations of the ejector. Calculated ejector outlet pressures for certain system setpoints were lower than the assumed flash tank pressure in the base CO_2 model leading to an additional assumption for this architecture that the MT expansion valve can handle the lower pressure differential between the MT evaporator and calculated flash tank pressures. The ejector calculations were performed using relationships outlined by Kornhauser (1990) and Bissolo (2015).

5. MODEL VALIDATION

For the base CO_2 architecture, several resources exist in the form of both research papers and manufacturer software. Mitsopoulos *et al.* (2019) replicated COP versus ambient temperature plots done by Tsamos *et al.* (2017) for a base transcritical CO_2 booster system. Comparing the present model to the findings of Mitsopoulos *et al* and Tsamos *et al* yielded deviations of 0-5% from the literature values as seen in Figure 3. The present work R-513A model results were also included in this plot as a reference.

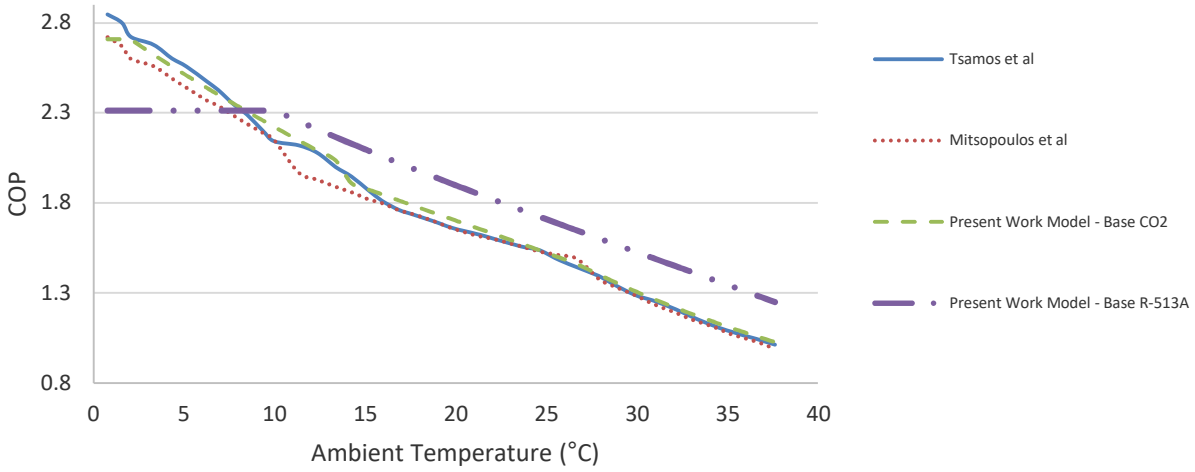

Figure 3: Model comparison using Mitsopoulos equations

6. DISCUSSION OF RESULTS

For each architecture studied, total compressor power at a given condensing condition was multiplied by the number of hours in the associated temperature bin for a given geographic location. The number of kilowatt-hours per year required to run the refrigeration system was then determined through the summation of all temperature bins for a given location. Comparisons were made between the base air-cooled R-513A booster, the base air-cooled CO_2 transcritical booster, the R-513A booster with adiabatic condenser, and the CO_2 transcritical booster with parallel compression, ejectors, and adiabatic condenser.

Compressor energy versus ambient temperature was plot for each location as seen in the profile for Miami, Florida, International Airport below.

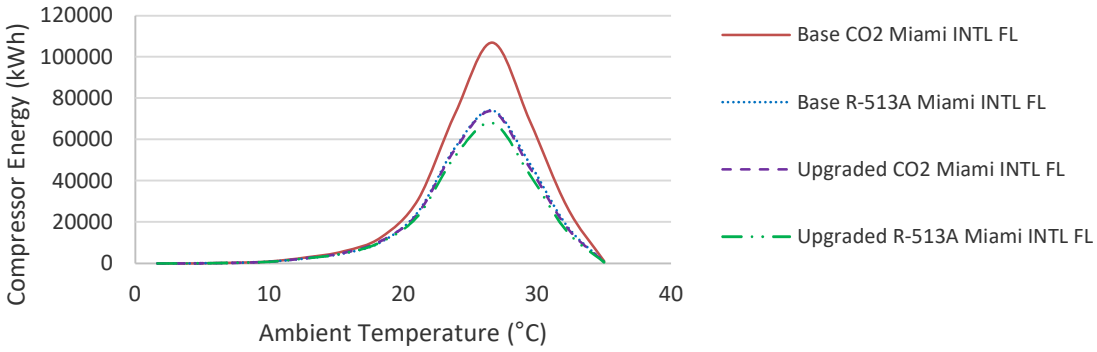

Figure 4: Miami, FL Compressor Energy versus Ambient Temperature

Dry bulb bin temperatures in Miami range from 1.7°C (35°F) to 35°C (95°F). As expected, the base CO_2 system performed poorly in this higher ambient climate. The use of upgrades like parallel compressors, ejectors, and an adiabatic condenser brought the CO_2 system performance much closer to the base R-513A booster. However, upgrading the condenser on the R-513A system to an adiabatic condenser and assuming a 10°C (50°F) minimum condensing temperature caused the upgraded R-513A booster to utilize less energy than the upgraded CO_2 system.

To show the contrast between climate zones, compressor energy versus ambient temperature was also plot using weather data from the international airport in Minot, North Dakota.

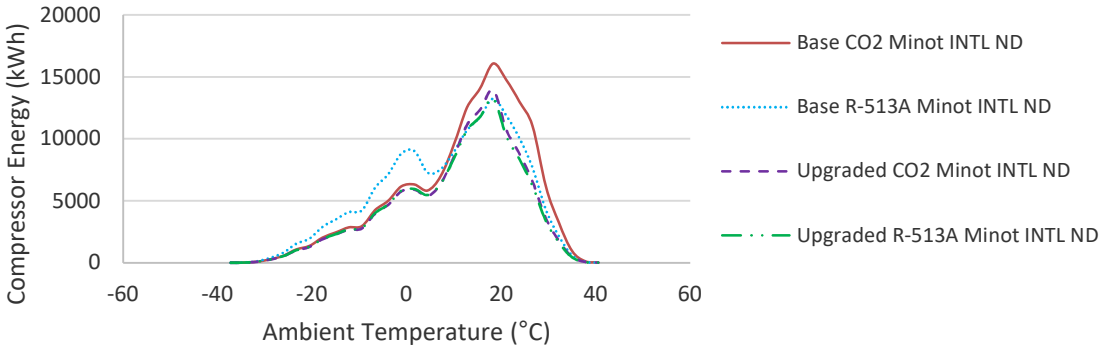

Figure 5: Minot, ND Compressor Energy versus Ambient Temperature

Dry bulb bin temperatures in Minot range from -37.2°C (-35°F) to 40.6°C (105°F). In contrast to the temperature distribution of Miami, the Minot plot was not clear as to which system used less energy in a year. After integrating these curves, however, it was found that the upgraded R-513A system outperformed all others.

The next comparison made was system COP versus ambient temperature. While CO_2 may exhibit significantly higher COP values at lower ambient temperatures, it is important to study the range of temperatures that is experienced in a given location and the coincident hours that are experienced at each temperature within that range.

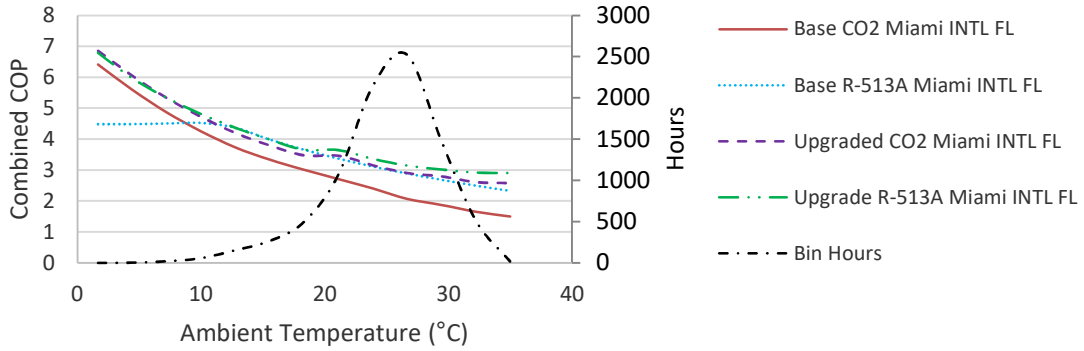

Figure 6: Miami, FL COP versus Ambient Temperature

Within the range of ambient temperatures in Miami, the base R-513A system had an average COP of 3.61 while the base CO_2 system average COP was 3.34. Most of the time, however, temperatures are between 21.1°C (70°F) and 32.2°C (90°F). When specifically viewing performance in this range, the difference in average COP became more pronounced in favor of R-513A.

Minot, having a wider temperature range and different temperature profile, was again difficult to visualize which system was better simply by looking at the COP versus ambient temperature plot. Integrating these curves yielded the same conclusion as Miami with the upgraded R-513A booster system using the least energy.

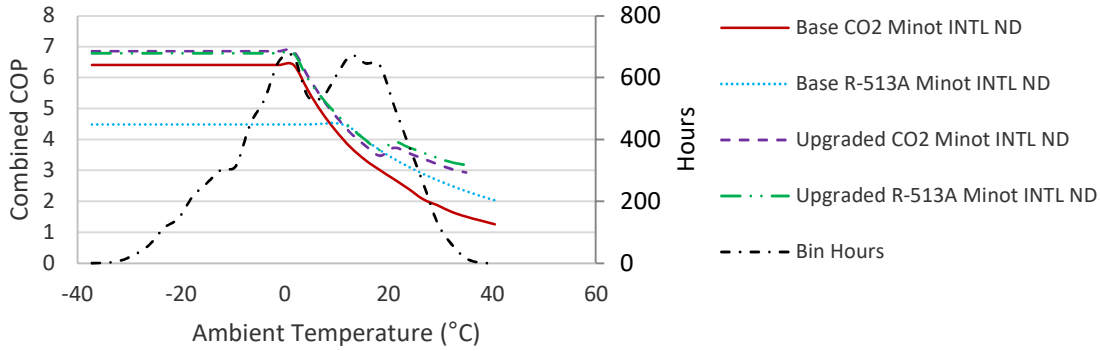

Figure 7: Minot, ND COP versus Ambient Temperature

To visually depict the performance of each system type in all climate zones, a plot of system energy usage (kWh) for a year of operation was generated. Regardless of location, the trend of energy usage between system types remained the same. Colder climates resulted in competitive performance of the base CO_2 system while warmer climates showed significantly increased CO_2 energy consumption. Adding parallel compression, ejectors, and an adiabatic condenser to the CO_2 system resulted in improved performance in all climate zones when compared to the base R-513A system. However, the upgraded R-513A booster system used less energy annually than the upgraded CO_2 system.

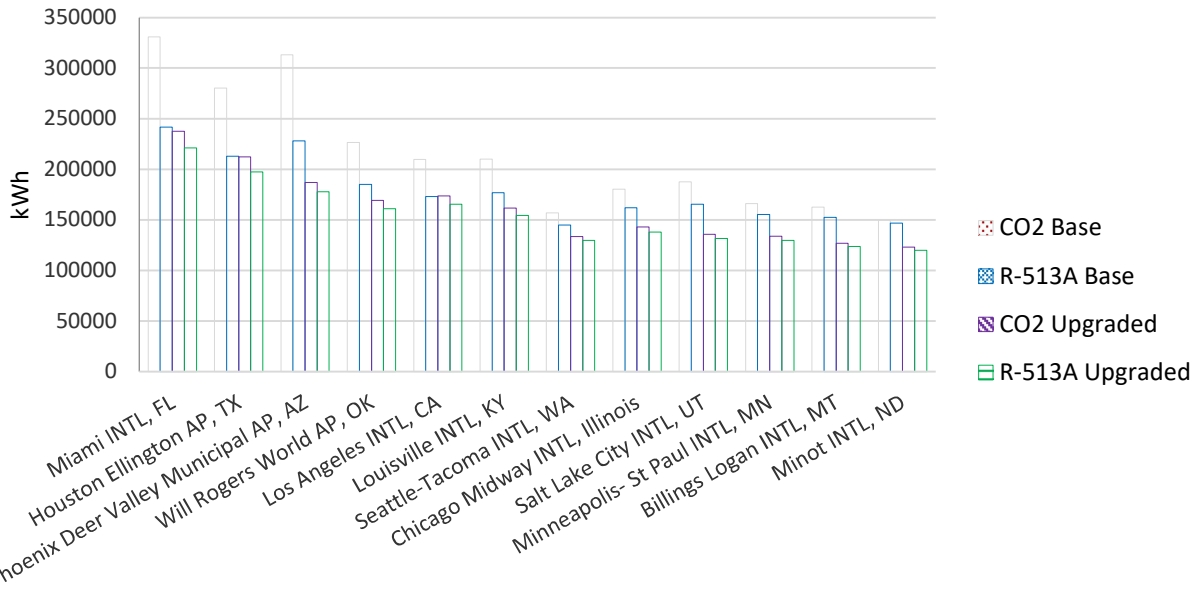

Figure 8: Yearly kWh by Location

8. CONCLUSIONS

Four different booster architectures were studied: an air-cooled R-513A booster system; an air-cooled CO_2 booster; a R-513A booster with an adiabatic condenser; and a CO_2 booster with a parallel compressor, ejector, and adiabatic condenser. When comparing the base cases, R-513A proved to be a more energy efficient cycle than CO_2. Adding parallel compression, ejectors and adiabatic condensers to CO_2 helped increase the thermodynamic efficiency, especially in warmer climates. However, it was demonstrated that the R-513A booster with an adiabatic condenser was the refrigeration architecture with the lowest energy usage across twelve different climate zones. Further development would include modifying the low and medium temperature load ratios, considerations for other architectures such as cascades or secondary loops, and investigations into heat recovery and mechanical subcooling.

NOMENCLATURE

Booster	The use of a LT compressor to lift the LT evaporator exit stream to the MT evaporator outlet pressure allowing both LT and MT evaporators to exist in the same circuit.
Gas Cooler	Term used for a CO_2 condenser at operation above the critical point.
Transcritical	Operation of a refrigerant in a system both above (supercritical) and below (subcritical) its critical point.
AR5	Intergovernmental Panel on Climate Change (IPCC) fifth assessment report

REFERENCES

ASHRAE (2017). *Weather Data Viewer* (Version 6.0) [CD-ROM].

Bhatia, A. Heat Rejection Options in HVAC Systems. *Continuing Education and Development Inc.* (2014).

Bissoli S. Future CO2 refrigeration systems for hot climates. *DTU Department of Mechanical Engineering Master Thesis*. (2015).

Emerson Climate Technologies. Commercial CO2 Refrigeration Systems Guide for Subcritical and Transcritical CO2 Applications. (2014).

Faramarzi R.T., Walker D.H. Investigation of Secondary Loop Supermarket Refrigeration Systems. *California Energy Commission*. (2004).

Ge Y.T., Tassou S.A. Performance evaluation and optimal design of supermarket refrigeration systems with supermarket model "SuperSim". Part II: Model applications. *International Journal of Refrigeration 34* (2010) 540-549.

Janna, W.S. (2010). *Design of Fluid Thermal Systems.* Stamford, CT: Cengage Learning.

Kornhauser A.A. The Use of an Ejector as a Refrigerant Expander. *International Refrigeration and Air Conditioning Conference* (1990). Paper 82.

Lemmon, E.W., Bell, I.H., Huber, M.L., McLinden, M.O. NIST Standard Reference Database 23: Reference Fluid Thermodynamic and Transport Properties-REFPROP, Version 10.0, National Institute of Standards and Technology, Standard Reference Data Program, Gaithersburg, 2018.

Liu F. Review on Ejector Efficiencies in Various Ejector Systems. *International Refrigeration and Air Conditioning Conference* (2014). Paper 1533.

Mitsopoulos G., Syngounas E., Tsimpoukis D., Bellos E., Tzivanidis C., Anagnostatos S. Annual performance of a supermarket refrigeration system using different configurations with CO_2 refrigerant. *Energy Conversion and Management: X 1* (2019) 100006.

Nelson C., Reis C., Nelson E., Armer J., Arthur R., Heath R., Rono J. Refrigeration Playbook: Natural Refrigerants Selecting and Designing Energy-Efficient Commercial Refrigeration Systems That Use Low Global Warming Potential Refrigerants. (2015).

Sarkar J. Ejector enhanced vapor compression refrigeration and heat pump systems – A review. *Renewable and Sustainable Energy Reviews 16* (2012) 6647-6659.

Saunders M., Knapke M., Patenaude A. Implementation of Low Condensing Refrigeration. *Emerson Climate Technologies Making Sense Webinar Series*. (2013).

Shilliday J.A. Investigation and Optimization of Commercial Refrigeration Cycles Using the Natural Refrigerant CO_2. *School of Engineering and Design, Brunel University.* (2012).

Sharma V., Fricke B., Bansal P. Comparative Analysis of Various CO2 Configurations in Supermarket Refrigeration Systems. *International Journal of Refrigeration*. (2014).

Tsamos K.M., Ge Y.T., Santosa I., Tassou S.A., Bianchi G., Mylona Z. Energy analysis of alternative CO_2 refrigeration system configurations for retail food applications in moderate and warm climates. *Energy Conversion and Management 150* (2017) 822-829.

Walker D. Development and Demonstration of an Advanced Supermarket Refrigeration/HVAC System. *Oak Ridge National Laboratory.* (2001).

Zhang M. Energy Analysis of Various Supermarket Refrigeration Systems. *International Refrigeration and Air Conditioning Conference* (2016). Paper 856.

ACKNOWLEDGEMENT

Special thanks to Ambica Pegallapati, Josh Hughes, Jason Juhasz, and Luke Simoni for their consultation in the development of these models.